

**A Family of Supramolecular Frameworks of Polyconjugated Molecules Hosted in Aromatic Nanochannels\*\***

Piero Sozzani,\* Angiolina Comotti, Silvia Bracco, and Roberto Simonutti

Organic molecules that contain extended conjugated  $\pi$  systems are an important class of active molecules, which show a number of attractive photochemical and electro-optical properties: they have applications as optical and electronic materials for photonics and data storage, and as semiconductors and probes in biological media.<sup>[1]</sup> Their inclusion in solid matrices extends the range of thermal stability, provides protection from chemical damage and improves their processability. Organized materials used as hosts are of particular interest, since they can transfer the benefits of their peculiar topological properties and modulate the functions of active molecules.<sup>[2]</sup> The application of the principles of self-assembly and crystal engineering<sup>[3]</sup> permits the manipulation of conjugated molecules through new interactions and the shaping of specific nanoscale environments in a way that mimics the control exerted by proteins on biological light receptors.<sup>[4]</sup> Noncovalent soft interactions are enough to bring about the spontaneous aggregation of host and guest molecules, even if they are very different in mass and their chemical nature. The tunability of the constraints and the variety of groups that can be involved in the weak interactions indicates a strategy that, besides modulating guest dynamics and conformations, allows us to explore a wide variety of intermolecular interactions.

The tris(*o*-phenylenedioxy)cyclotriphosphazene (TPP) molecule exhibits high  $D_{3h}$  symmetry, that disfavors close packing and promotes the formation of host–guest adducts.<sup>[5]</sup> The versatility of TPP is such that it has intriguing properties; it can self-assemble, and can form a nanoporous material with permanent nanochannels of 0.5 nm in diameter that can absorb molecules from the gas phase.<sup>[6]</sup> Herein we show that a variety of linear  $\pi$ -conjugated molecules can be encapsulated in infinite nanochannels lined with aromatic groups, which offer tailored surroundings of weak interactions. Self-organization with TPP resulted in nanostructured adducts of exceptional stability in which polyconjugated molecules sit aligned in the parallel nanochannels of the crystalline framework (Figure 1). The novel host–guest architectures with

[\*] Prof. P. Sozzani, Dr. A. Comotti, Dr. S. Bracco, Dr. R. Simonutti  
Department of Materials Science  
University of Milano-Bicocca  
Via R. Cozzi 53, 20125 Milan (Italy)  
Fax: (+39) 02-6448-5400  
E-mail: piero.sozzani@unimib.it

[\*\*] This work was partially supported by MIUR. The authors would like to thank Prof. M. C. Gallazzi and Dr. Carla Mattarini for their help in the synthesis of some molecules.



Supporting information for this article is available on the WWW under <http://www.angewandte.org> or from the author.

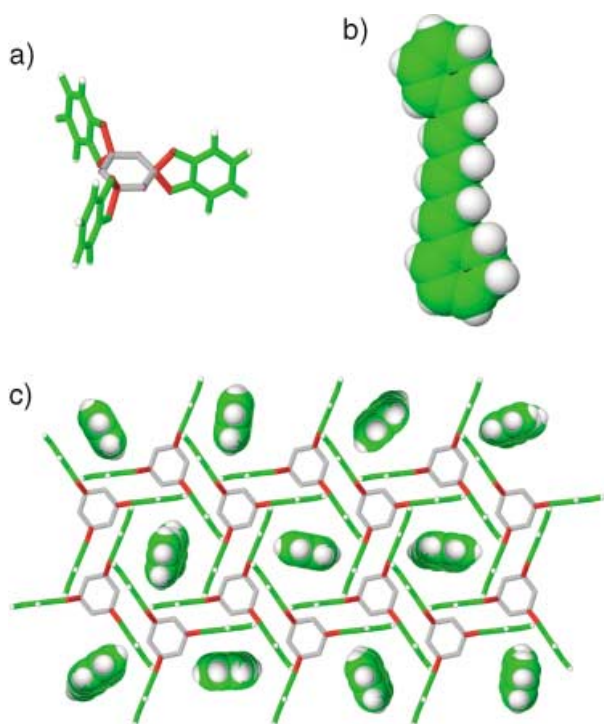


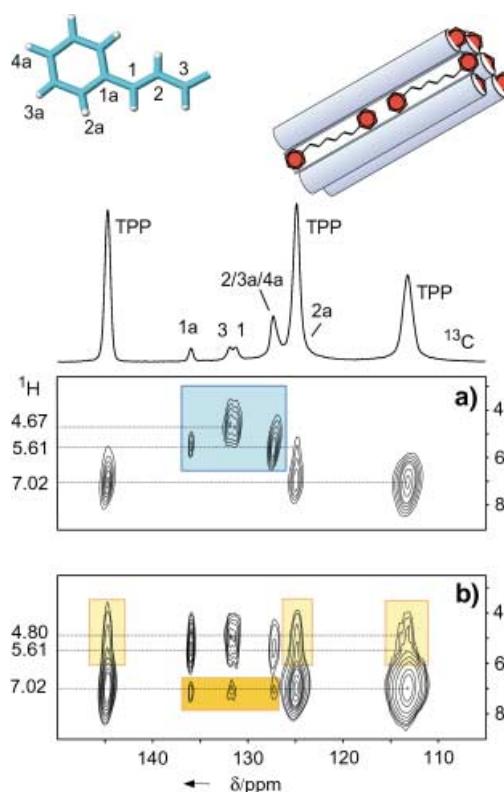
**Figure 1.** An example of adducts of tris(*o*-phenylenedioxy)spirocyclotriphosphazene (TPP) with polyconjugated molecules (green: carbon; white: hydrogen; violet: phosphorous; gray: phosphazenic ring). a) Side view of TPP (ball-and-stick mode) as arranged in the hexagonal crystal cell of the compounds **1–10**. b) Space-filling mode of *trans,trans,trans*-1,6-diphenyl-1,3,5-hexatriene molecule. c) Projection of the hexagonal crystalline adduct of TPP with guest molecules viewed along the channel axis (*c* axis). The guest molecules are aligned uniaxially along the nanochannels.

conjugated molecules are sustained by a diffuse network of  $\text{CH}\cdots\pi$  and  $\pi\cdots\pi$  interactions that, through cooperation, improve the robustness of the supramolecular adducts. The stabilizing interactions were recognized by using advanced high-resolution 2D hydrogen–carbon solid-state NMR techniques, now available for elucidating the structure and dynamics of large supramolecular assemblies.<sup>[7]</sup> Linear conjugated molecules that contain various chains of building blocks (i.e., double bonds, phenyl and thiophene rings) could be included to form the adducts **1–10** (Table 1).

The self-assembly process is evidenced by the spontaneous formation of the supramolecular adducts, shown in the differential scanning calorimetry (DSC) traces by exotherms that occur simultaneously with, or subsequently to, the melting of the guests (Supporting Information). The congruent melting of the adducts are at temperatures higher than that of both the matrix (250°C) and the guests. Thus, the range of thermal stability of the nanostructured materials **1–10** extends up to 310°C ( $\Delta H_m \approx 90 \text{ J g}^{-1}$ ), 100–200°C higher than the melting points of the guests.<sup>[8]</sup> Their crystal structures show a virtually identical hexagonal architecture dictated by the host (space group  $P6_3/m$ ), as determined by the resolution of single-crystal structures of selected samples and the simulation of the powder-diffraction profiles<sup>[9]</sup> (the crystallographic data and refinements are given in the Supporting

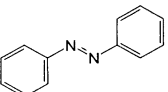
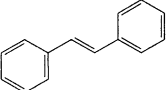
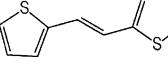
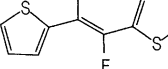
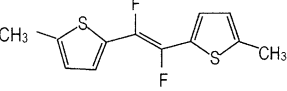
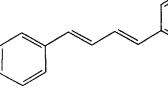
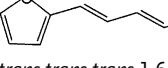
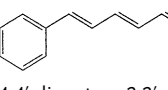
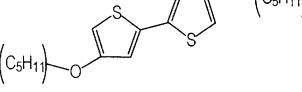
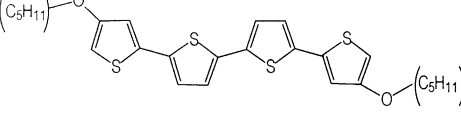
Information). Concerning the guest atoms, Fourier-difference synthesis could determine a residual electron-density distribution diffused along the nanochannels without any specificity, thus indicating the occurrence of static or dynamic disorder of the guests in the incommensurate structures. Adducts **1–10** and the bulk guests were characterized by  $^1\text{H}$ ,  $^{13}\text{C}$ , and  $^{31}\text{P}$  MAS NMR spectroscopy at a spinning speed of 15 kHz (chemical-shift assignments are given in the Experimental Section and Supporting Information). The low multiplicity of the matrix signals indicates the high symmetry of the TPP molecule in the hexagonal honeycomb structure, which is consistent with results from X-ray diffraction (Figure 1).

Advanced 2D NMR spectroscopy experiments based on fast magic-angle spinning and Lee–Goldburg decoupling (Supporting Information) can reduce hydrogen–hydrogen homonuclear coupling and result in high resolution in the hydrogen region of the spectrum. The resolution and sensitivity in 2D reduces the overlapping of signals so that isotope labeling is not required to detect intermolecular interactions.<sup>[7]</sup> Analysis of the compound with diphenylhexatriene (**8**) at 1 ms cross-polarization time results in a 2D  $^1\text{H}$ ,  $^{13}\text{C}$  HETCOR Lee–Goldburg NMR spectrum with well separated host and guest signals (Figure 2a); cross signals of the guest molecules are indicated by the blue area. The remarkable resolution shows the hydrogen signals assigned to the



**Figure 2.** Contour plots of 2D phase-modulated Lee–Goldburg PMLG decoupled heteronuclear ( $^1\text{H}$ ,  $^{13}\text{C}$ ) dipolar correlation spectra of compound **8**. The spectra were performed in a magnetic field of 7.04 T by using a spinning speed of 15 kHz. Ramped cross-polarization times of a) 1 ms (blue area: guest–guest cross signals) and b) 5 ms (yellow area and orange area: guest–TPP and TPP–guest cross signals, respectively) were applied.

**Table 1:** Guest molecules and their adducts with TPP 1–10 along with their melting properties.

	Name and structural formula of the guest molecules <sup>[a]</sup>	$T_m$ pure [°C] <sup>[b]</sup>	$T_m$ of the adduct [°C] <sup>[b]</sup>
1	<i>trans</i> -azobenzene 	68	266
2	<i>trans</i> -stilbene 	125  ≈ 97 %	275
3	<i>trans</i> -1,2-di(2-thienyl)-ethylene 	134  > 98 %	283
4	<i>trans</i> -1,2-difluoro-1,2-di(2-thienyl)-ethylene 	94	284
5	<i>trans</i> -1,2-difluoro-1,2-di(5-methyl-2-thienyl)-ethylene 	86  > 98 %	290 <sup>[c]</sup>
6	<i>trans,trans</i> -1,4-diphenyl-1,3-butadiene 	153  ≥ 99 %	289 <sup>c</sup>
7	1,4-di(2-thienyl)-1,3-butadiene 	173	301
8	<i>trans,trans,trans</i> -1,6-diphenyl-1,3,5-hexatriene 	203  ≥ 99 %	309 <sup>c</sup>
9	4,4'-dipentoxo-2,2'-dithiophene 	52	296 <sup>c</sup>
10	4,4'''-dipentoxo-2,2':5',2'':5'',2''':5'''-tetrathiophene 	119	313 <sup>c</sup>

[a] The guest molecules are listed according to molecular masses. [b] The accuracy of the melting point is  $\pm 1^\circ\text{C}$ ; the calorimetric traces of the adducts are reported in the Supporting Information. [c] The adduct was also prepared by crystallization from *o*-xylene solution.

polyene chains ( $\delta_{\text{H}} = 4.7$  ppm) and the aromatic heads ( $\delta_{\text{H}} = 5.6$  ppm) of the guest.

The nanochannels of TPP develop aromatic walls with the phenylenedioxy groups facing the guests, which generates a notable upfield shift of about 2 ppm ( $\Delta = \delta_{\text{adduct}} - \delta_{\text{liquid}} = -2$  ppm) due to the diamagnetic susceptibility produced by the host paddles wrapping around the confined guests. Longer cross-polarization times (5 ms) result in new correlation signals (Figure 2b) that pertain to through-space intermolecular interactions between TPP and diphenylhexatriene nuclei,

thus indicating an intimate relationship among the assembly components.

In the 2D HETCOR experiment, proton magnetization evolves during  $t_1$  under its chemical-shift Hamiltonian and then is transferred to the nearby carbon atoms by cross polarization: the intensity of the correlation signal is a measurement of the distance  $d$  according to the scaling law of  $1/d^6$ . The effectiveness of the transfer highlights the short hydrogen-to-carbon distances. Compounds **2** and **6**, as well as the diazobenzene adduct **1**, show similar host-guest interactions and diamagnetic upfield shifts. The adduct **9** formed with a dithiophene derivative that bears the pentoxo side chains is an example of one of the thiophene-containing compounds (**3**, **4**, **5**, **7**, **9**, and **10**). Selected 2D  $^1\text{H}$ ,  $^{13}\text{C}$  HETCOR spectra are shown in Figure 3.

The exceptional resolution in the hydrogen domain and the large magnetic susceptibility was exploited to understand the precise topology of the hydrogen atoms in the adduct. In a control experiment on the pure bulk material, only intramolecular correlations of protons to vicinal carbon atoms were active (Figure 3a): an exception being methyl and  $\gamma$ -methylene protons that show intermolecular correlations with thiophene ring carbon (C3 and C5), since the *trans* aliphatic chains point towards the thiophene ring of a vicinal molecule in the herringbone arrangement<sup>[10]</sup> (Figure 3c). In contrast, the 2D spectrum of adduct **9** (Figure 3b) shows a multiplicity of host-guest interactions and a strong upfield shift of the guest signals in the carbon and hydrogen dimension (compare projections of Figure 3b to Figure 3a). The dramatic shifts of the hydrogen-atom signal of  $-1.8/-2.2$  ppm have such an influence in the  $^1\text{H}$  MAS NMR spectrum (Figure 3e) that methyl protons resonate upfield to TMS at  $\delta_{\text{H}} = -1.1$  ppm, methyleneoxy protons move from  $\delta_{\text{H}} = 3.6$  to 1.8 ppm and thiophene protons at  $\delta_{\text{H}} = 4.10$  ppm are prevented from overlapping with the TPP signal.<sup>[11]</sup>

The marked upfield shifts are observed here for the first time in the spectrum of the polyconjugated molecules embedded in aromatic nanochannels, and the 2D cross signals are a clear demonstration of the intimate relationship of the guest with the host aromatic groups. The strong magnetic susceptibility, derived from the TPP aromatic paddles, permits the exact determination of the distance of a probe atom from the phenylenedioxy ring (Figure 4). Nucleus-independent chemical-shift maps give the calculated chemical shifts in the region around the aromatic ring, as derived from

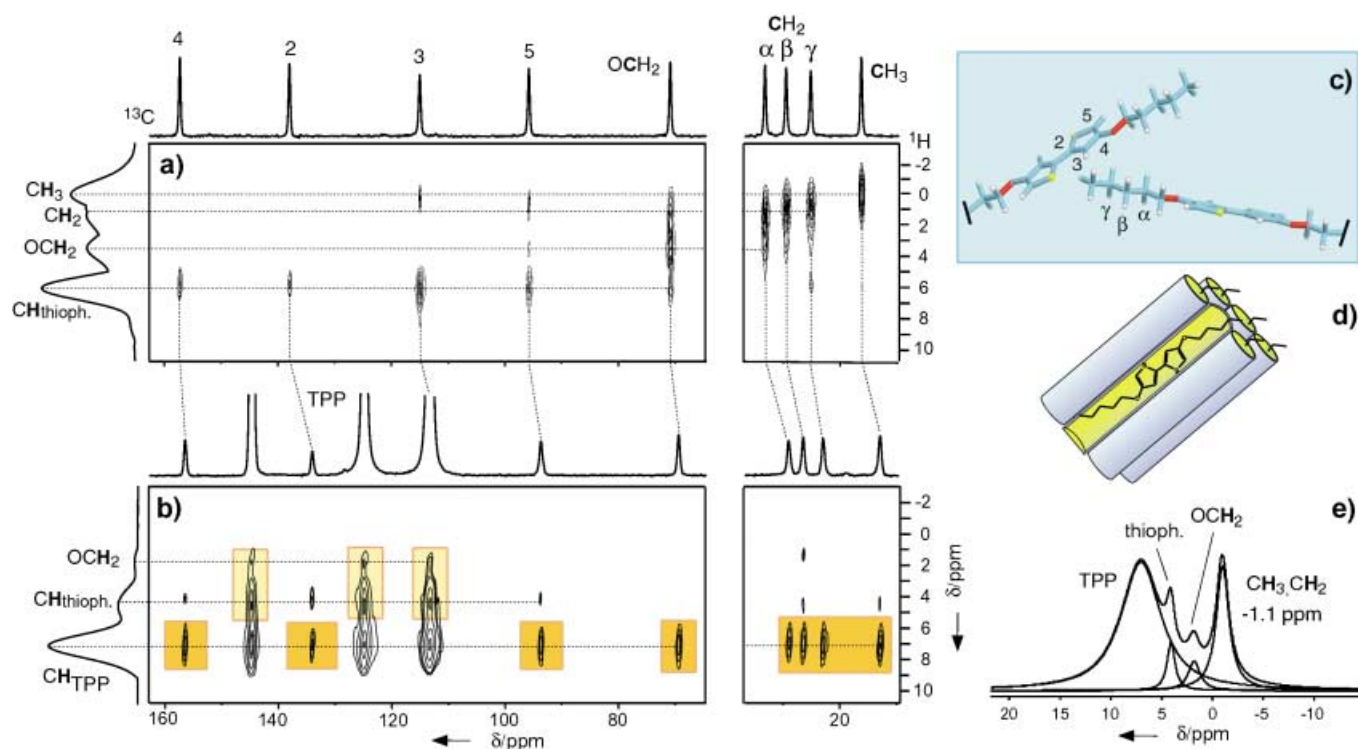


**Figure 3.** Contour plots of 2D PMLG decoupled heteronuclear ( $^1\text{H}$ ,  $^{13}\text{C}$ ) dipolar correlation spectra of a) the 4,4'-dipentoxo-2,2'-dithiophene and b) compound **9**. The spectra were performed in a magnetic field of 7.04 T by using a spinning speed of 15 kHz. Ramped cross-polarization times of a) 1 ms and b) 5 ms were applied (yellow and orange areas: guest-TPP and TPP-guest cross signals). c) A view of two molecules in the monoclinic unit cell, space group  $P2_1/c$   $a = 9.823(1)$ ,  $b = 11.942(2)$ ,  $c = 7.885(1)$  Å,  $\beta = 90.13^\circ(2)$  (blue: carbon; yellow: sulfur; white: hydrogen). d) Schematic picture of the 4,4'-dipentoxo-2,2'-dithiophene confined to the aromatic nanochannels. e)  $^1\text{H}$  MAS NMR spectrum of **9** obtained with a spinning speed of 15 kHz.

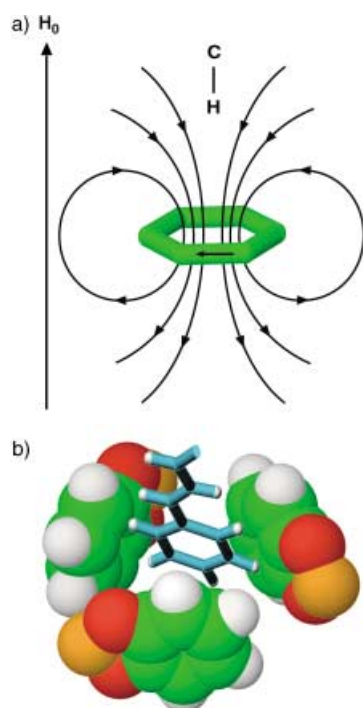


**Figure 4.** a) Topology of guest hydrogen atoms located at 2.5 Å above the plane of the benzene rings: the ring currents generate an upfield shift of 2 ppm. b) An example of a polyconjugated guest molecule encapsulated in the nanochannel and surrounded at a close contact by three aromatic paddles of the TPP host.

the electronic current density generated by the main magnetic field.<sup>[12]</sup> Proton resonances shifted 2 ppm upfield indicate the topology of the guest hydrogen atoms above the plane of benzene rings at a distance of 2.5 Å (Figure 4a).<sup>[13]</sup> Short intermolecular distances, such as those determined, imply close contact between the  $\pi$ -electron clouds and hydrogen atoms, and favorable Van der Waals interactions. Both theoretical studies and the survey of a number of crystal structure determinations have established that energy minima occur at distances of hydrogen atoms from the center of aromatic rings of between 2.5 and 2.8 Å.

The  $\text{CH}\cdots\pi$  arrangements account for about 2 kcal mol $^{-1}$  of energy.<sup>[14]</sup> Recently, energy minima of 2.5 kcal mol $^{-1}$  were accurately determined for benzene dimers in the favorable T-shaped and slipped-parallel arrangements. At the minima, the intermolecular distance of CH hydrogen atoms from the aromatic center is 2.5 Å, as in the present case.<sup>[15]</sup> The XRD structural resolution, although unable to detect the exact location of the guests, describes the crystal buildings in which the guests are encapsulated. The existence of  $\text{CH}\cdots\pi$  interactions is compatible with the size of the 5 Å nanochannels that are recognizable in the crystal structure. Three contiguous phenylenedioxy rings are present at each cross section of TPP structure (Figure 4b) and another three, related by a 6 $_3$  screw axis, are found on the next TPP layer along the channel.

Thus, both the aromatic and aliphatic CH groups of the guest find, with high probability, any of the  $\pi$ -receptors lining

the walls and move to vicinal receptors through low activation energies. Multiple CH $\cdots\pi$  interactions simultaneously sustain the architecture, and make a notable contribution to the exothermic self-assembly. Melting enthalpies evaluated by DSC and referenced to one mole of TPP, give values of 6 kcal mol $^{-1}$  for bulk TPP in the nanoporous modification (host–host interactions) and about 12 kcal mol $^{-1}$  for the adducts (host–host and host–guest interactions).<sup>[16]</sup> Since the host arrangement is the same in the bulk nanoporous modification as in the adducts, the difference in enthalpy is mostly due to the host–guest interactions, accounting for 2 kcal mol $^{-1}$  per each TPP paddle involved in CH $\cdots\pi$  interactions. Also, the conformational arrangement of the guests differs from that of the bulk by as much as it does from that of the solutions. Conformations contribute to additional upfield shifts, even reaching on some carbon atoms a shift value of –4 ppm with respect to the bulk. The large shift must be ascribed to the  $\gamma$ -*gauche* shielding effect<sup>[17]</sup> added with the same sign to the magnetic susceptibility. In the nanostructured environment, although the molecules are squeezed to elongated shapes, departure from *trans* conformations is largely tolerated, since the guests are softly embraced within an organized environment. In fact, the interactions are loose enough to permit a diffusional spinning motion of the guests within the nanochannels, which is consistent with carbon spin-lattice relaxation times of 10–30 s in the extreme narrowing regime of motions, with correlation times of  $\tau_c < 10^{-8}$  s for all the guests.<sup>[18]</sup> Interestingly, entropy decreases moderately while weak interactions lead to the formation of host–guest complexes: if the host–guest interactions were strong and tight enough to impede librations and torsions of the guests, the entropy loss would be also greater, thus leading the enthalpy/entropy balance to compensate, without gaining much advantage through thermal stability.<sup>[19]</sup> Thus, guest dynamics concur with the favorable host–guest interactions resulting in a surprising overall stabilization, which allows adducts to exist at high temperatures.

In summary, linear  $\pi$ -conjugated molecules have been engineered in unique supramolecular structures in such a way as to be completely surrounded by aromatic groups. The molecules are confined by self-assembly within a crystalline honeycomb network and have uniform alignment along the crystallographic *c* axis, with the stimulating perspective of orienting anisotropically the active molecules in thermally stable single crystals. Unconventional NMR spectroscopic techniques were able to localize, with rare accuracy, the hydrogen atoms involved in weak hydrogen-atom– $\pi$  interactions and found the central motif common to the novel nanostructures, that is, the organization of  $\pi$  receptors wrapping about the guests and sustaining a diffuse network of weak  $\pi\cdots\pi$  and aliphatic CH $\cdots\pi$  interactions. Weak host–guest interactions form collectively a robust, exceptionally stable, architecture that nevertheless provides a soft environment for the guest: an ideal locus at which the encapsulated molecules are balanced between freedom and constriction. Interestingly, the infinite fully aromatic nanochannels, shaped by the host, resemble carbon nanotubes<sup>[20]</sup> with the aromatic rings parallel to the channel axis. The novel series of supramolecular adducts contribute to the evolution of new generations of 1D

ordered assemblies of important families of functional molecules with the strategy of exploiting weak interactions to modulate the molecular arrangements and functions.

### Experimental Section

TPP was synthesized according to a reported procedure.<sup>[6c]</sup> Compounds **1–10** were prepared either by crystallization from *o*-xylene solutions of TPP (0.01 mole L $^{-1}$ ) and guest molecules or by heating intimately mixed guest and TPP powders above the melting point of the guests (host–guest weight ratio of about 6:1); *o*-xylene was previously purified by *n*-nonane impurities by using molecular sieves and TPP itself as entrapment agent of linear alkanes. No inclusion compound with 3,3'-dipentoxo-2,2'-dithiophene is formed due to the steric hindrance of the molecule.

Received: December 8, 2003

Revised: February 27, 2003 [Z53479]

**Keywords:** conjugation · crystal engineering · nanostructures · NMR spectroscopy · supramolecular chemistry

- [1] a) D. Fichou, *Handbook of Oligo- and Polythiophenes*, Wiley-VCH, New York, **1999**; b) D. C. Rodenberger, J. R. Heflin, A. F. Garito, *Nature* **1992**, 359, 309–311; c) Y. Cao, I. D. Parker, G. Yu, C. Zhang, A. J. Heeger, *Nature* **1999**, 397, 414–417; d) R. H. Friend, R. W. Gymer, A. B. Holmes, J. H. Burroughes, R. N. Marks, C. Taliani, D. D. C. Bradley, D. A. Dos Santos, J. L. Brédas, M. Lögdlund, W. R. Salaneck, *Nature* **1999**, 397, 121–128; e) B. Crone, A. Dodabalapur, Y.-Y. Lin, R. W. Filas, Z. Bao, A. LaDuca, R. Sarpeshkar, H. E. Katz, W. Li, *Nature* **2000**, 403, 521–523; f) W. T. Mason, *Fluorescent and Luminescent Probe for Biological Activity*, Academic Press, New York, **1999**; g) T. Besanger, Y. Zhang, J. D. Brennan, *J. Phys. Chem. B* **2002**, 106, 10535–10542.
- [2] A number of hosts have been proposed for confining the conjugated molecules to nanochannels: zeolites, cyclodextrins, mesoporous materials, and clathrates: a) V. Ramamurthy, J. V. Caspar, D. F. Eaton, E. W. Kuo, D. R. Corbin, *J. Am. Chem. Soc.* **1992**, 114, 3882–3892; b) G. Calzaferri, S. Huber, H. Maas, C. Minkowski, *Angew. Chem.* **2003**, 115, 3860–3888; *Angew. Chem. Int. Ed.* **2003**, 42, 3732–3758; c) M. N. Berberan-Santos, P. Choppinet, A. Fedorov, L. Jullien, B. Valeur, *J. Am. Chem. Soc.* **2000**, 122, 11876–11886; d) G. Li, L. B. McGown, *Science* **1994**, 264, 249–251; e) C.-G. Wu, T. Bein, *Science* **1994**, 264, 1757–1759; f) S. Spange, *Angew. Chem.* **2003**, 115, 4568–4570; *Angew. Chem. Int. Ed.* **2003**, 42, 4430–4432; g) T. Aida, K. Tajima, *Angew. Chem.* **2001**, 113, 3919–3922; *Angew. Chem. Int. Ed.* **2001**, 40, 3803–3806; h) G. Macchi, F. Meinardi, R. Simonutti, P. Sozzani, R. Tubino, *Chem. Phys. Lett.* **2003**, 379, 126–131; i) R. Hoss, O. König, V. Kramer-Hoss, U. Berger, P. Rogin, J. Hulliger, *Angew. Chem.* **1996**, 108, 1774–1776; *Angew. Chem. Int. Ed. Engl.* **1996**, 35, 1664–1666.
- [3] Special Issue “Supramolecular Chemistry and Self-Assembly”: *Science* **2002**, 295, 2400–2421; in particular: J.-M. Lehn, *Science* **2002**, 295, 2400–2403.
- [4] G. Gröbner, I. J. Burnett, C. Glaubitz, G. Choi, A. J. Mason, A. Watts, *Nature* **2000**, 405, 810–813; C. Dugave, L. Demange, *Chem. Rev.* **2003**, 103, 2475–2532.
- [5] a) T. Kobayashi, S. Isoda, K. Kubono in *Comprehensive Supramolecular Chemistry*, Vol. 6 (Eds.: J. L. Atwood, J. E. D. Davies, D. D. MacNicol, F. Vögtle), Pergamon, Oxford, **1996**, pp. 399–419; b) H. R. Allcock, M. L. Levin, R. R. Whittle, *Inorg. Chem.* **1986**, 25, 41–47.

- [6] a) P. Sozzani, A. Comotti, R. Simonutti, T. Meersmann, J. W. Logan, A. Pines, *Angew. Chem.* **2000**, *112*, 2807–2810; *Angew. Chem. Int. Ed.* **2000**, *39*, 2695–2699; b) T. Meersmann, J. W. Logan, R. Simonutti, S. Caldarelli, A. Comotti, P. Sozzani, L. G. Kaiser, A. Pines, *J. Phys. Chem. A* **2000**, *104*, 11665–11670; c) A. Comotti, R. Simonutti, G. Catel, P. Sozzani, *Chem. Mater.* **1999**, *11*, 1476–1483; d) T. Hertzsch, S. Kluge, E. Weber, F. Budde, J. Hulliger, *Adv. Mater.*, **2001**, *13*, 1864–1867; e) A. Barbon, M. Bortolus, M. Brustolon, A. Comotti, A. Maniero, U. Segre, P. Sozzani, *J. Phys. Chem. B* **2003**, *107*, 3325–3331.
- [7] a) S. P. Brown, H. W. Spiess, *Chem. Rev.* **2001**, *101*, 4125–4155; b) E. Vinogradov, P. K. Madhu, S. Vega, *Chem. Phys. Lett.* **1999**, *314*, 443–450; c) P. Sozzani, S. Bracco, A. Comotti, I. Camurati, R. Simonutti, *J. Am. Chem. Soc.* **2003**, *125*, 12881–12893.
- [8] The process is efficient in selecting linear guests that can adopt extended geometries without lateral hindrance: other potential guests are excluded from the assembly, as is, for example, the case of 3,3'-dipentoxo-2,2'-dithiophene.
- [9] The single-crystal X-ray data were collected on an Oxford Xcalibur automated 4-circle diffractometer with  $\theta$  geometry equipped with CCD detector and a Mo-target X-ray tube operating at 50 kV and 30 mA with a radiation wave length  $\lambda$  of 0.71073 Å. The frames were integrated with the CrysAlis RED program of Oxford Diffraction. Absorption correction was applied by using the program SADABS. The structure was solved by direct methods, the subsequent difference Fourier synthesis and refinement by using the JANA2000 software package. X-ray data for **9**, crystal size 70  $\mu\text{m} \times 100 \mu\text{m} \times 120 \mu\text{m}$ , hexagonal, space group  $P6_3/m$ ,  $a = b = 11.627(1)$  Å,  $c = 10.084(1)$  Å,  $\gamma = 120^\circ$ ,  $Z = 2$ ,  $V = 1180.7(2)$  Å<sup>3</sup>,  $3.5^\circ < \vartheta < 32.3^\circ$ , a total of 912 frames were collected with a scan width of 1.9 deg in  $\omega$  and  $\varphi$  with an exposure time of 40 s per frame,  $T = 298$  K, 35419 measured reflections, 1365 ( $R_{\text{int}} = 0.070$ ) independent reflections,  $R_1 = 0.0748$ ,  $wR_2 = 0.0192$  for 10314 observed reflections with ( $I > 3\sigma$ ). GOF = 2.51, refinement method was full-matrix least-squares on  $F^2$ . X-ray data for **10**, crystal size 100  $\mu\text{m} \times 120 \mu\text{m} \times 150 \mu\text{m}$ , hexagonal, space group  $P6_3/m$ ,  $a = b = 11.674(1)$  Å,  $c = 10.073(1)$  Å,  $\gamma = 120^\circ$ ,  $Z = 2$ ,  $V = 1188.8(2)$  Å<sup>3</sup>,  $4.5^\circ < \vartheta < 32.2^\circ$ , a total of 1158 frames were collected with a scan width of 1.5 deg in  $\omega$  and  $\varphi$  with an exposure time of 40 s per frame,  $T = 298$  K, 40391 measured reflections, 1394 ( $R_{\text{int}} = 0.13$ ) independent reflections,  $R_1 = 0.0606$ ,  $wR_2 = 0.01147$  for 6467 observed reflections with ( $I > 3\sigma$ ). GOF = 0.86, refinement method was full-matrix least-squares on  $F^2$ . Simulated powder profiles as derived from single-crystal data reproduce the experimental X-ray powder patterns of all the compounds. Powder X-ray diffraction patterns of the compounds were recorded by using a Bruker D8 Advance diffractometer ( $\text{CuK}\alpha$  radiation) in the  $2\theta$  range 5 to  $60^\circ$ , with  $\Delta(2\theta) = 0.02^\circ$  and 4 s per step as counting time. The peaks are indexed as a hexagonal cell, space group  $P6_3/m$ . The least-squares refined unit-cell constants are the following: **1**:  $a = b = 11.710(6)$  Å,  $c = 10.11(1)$  Å,  $V = 1200.413$  Å<sup>3</sup>; **2**:  $a = b = 11.680(3)$  Å,  $c = 10.084(5)$  Å,  $V = 1191.389$  Å<sup>3</sup>; **3**:  $a = b = 11.661(2)$  Å,  $c = 10.077(2)$  Å,  $V = 1186.761$  Å<sup>3</sup>; **5**:  $a = b = 11.711(3)$  Å,  $c = 10.090(4)$  Å,  $V = 1198.326$  Å<sup>3</sup>; **6**:  $a = b = 11.701(3)$  Å,  $c = 10.094(5)$  Å,  $V = 1196.848$  Å<sup>3</sup>; **8**:  $a = b = 11.648(1)$  Å,  $c = 10.090(2)$  Å,  $V = 1185.541$  Å<sup>3</sup>. Further details are reported in the Supporting Information.
- [10] S. V. Meille, A. Farina, Bezziccheri, M. C. Gallazzi, *Adv. Mater.* **1994**, *6*, 848–851.
- [11] Also in the other adducts, for example, the adduct **10** (Supporting Information), the aromatic hydrogens of thiophene and TPP cross-correlate strongly with the carbon atoms of each other and the full hydrogen spectrum of the guest is noticeably shifted when the guest sits in the unusual aromatic environment.
- [12] a) P. von Ragué Schleyer, C. Maerker, A. Dransfeld, H. Jiao, N. J. R. Van Eikema Hommes, *J. Am. Chem. Soc.* **1996**, *118*, 6317–6318.
- [13] a) J. S. Waugh, R. W. Fessenden, *J. Am. Chem. Soc.* **1957**, *79*, 846–849; b) J. Canceill, L. Lacombe, A. Collet, *J. Am. Chem. Soc.* **1986**, *108*, 4230–4232; c) N. H. Martin, N. W. Allen III, K. D. Moore, L. Vo, *J. Mol. Struct. (Theochem)* **1998**, 161–166; d) A. Rapp, I. Schnell, D. Sebastiani, S. P. Brown, V. Percec, H. W. Spiess, *J. Am. Chem. Soc.* **2003**, *125*, 13284–13297.
- [14] a) M. Nishio, M. Hirota, Y. Umezawa in *The CH/ $\pi$  interaction. Evidence, nature and consequences*, Wiley, New York, **1998**; b) G. R. Desiraju, *Acc. Chem. Res.* **2002**, *35*, 565–573.
- [15] a) S. Tsuzuki, K. Honda, T. Uchimaru, M. Mikami, K. Tanabe, *J. Am. Chem. Soc.* **2002**, *124*, 104–112.
- [16] In elongated guests only a minor contribution is made by terminal guest–guest interaction along the nanochannel.
- [17] A. E. Tonelli, *Macromolecules* **1978**, *11*, 565–567.
- [18] Diphenylhexatriene molecules in adduct **8** show, for instance, a relaxation time of only 7 s for the quaternary carbon and less than 1 s for the inner polyene chain, thus indicating large librations and diffusional rotations about the channel axis. This observation is also true for condensed polythiophene rings because <sup>13</sup>C relaxation times  $T_1$  are about 10 s in the tetrathiophene and 30 s in dithiophene in the adducts **9** and **10**. Relaxation times measured at variable temperatures demonstrate that the motions are in the extreme narrowing regime: at lower temperatures the carbon relaxation times become longer.
- [19] a) A very recent survey of the literature discusses a large number of cases in host–guest chemistry in which the compatibility of weak interactions with large entropy in the solid is highlighted: K. N. Houk, A. G. Leach, S. P. Kim, X. Zhang, *Angew. Chem.* **2003**, *115*, 5020–5046; *Angew. Chem. Int. Ed.* **2003**, *42*, 4872–4897; b) A functional relationship was derived by Dunitz for quantifying enthalpy/entropy compensation during the formation of intermolecular adducts: J. D. Dunitz, *Chem. Biol.* **1995**, *2*, 709–712; c) M. S. Westwell, M. S. Searle, J. Klein, D. H. Williams, *J. Phys. Chem.* **1996**, *100*, 16000–16001.
- [20] X. Zhang, T. Liu, T. V. Sreekumar, S. Kumar, V. C. Moore, R. H. Hauge, R. E. Smalley, *Nano Lett.* **2003**, *3*, 1285–1288, and references therein.